International Journal of Geo-Information

MDPI

Article

Spatial and Temporal Changes and Influencing Factors of Capital Cities in Five Provinces of the Underdeveloped Regions of Northwest China

Yuanbao Feng [1,†], Yujun Ma [1,2], Wei Jia [1,2,*,†], Sifa Shu [1], Hongda Li [3] and Xiangyu Hu [1]

[1] Qinghai Provincial Key Laboratory of Physical Geography and Environmental Process, College of Geographical Science, Qinghai Normal University, Xining 810008, China; fyb@stu.qhnu.edu.cn (Y.F.); yujunma@qhnu.edu.cn (Y.M.); ssfily@stu.qhnu.edu.cn (S.S.); hxy@stu.qhnu.edu.cn (X.H.)
[2] Academy of Plateau Science and Sustainability, Qinghai Normal University, Xining 810008, China
[3] Qinghai Grassland Station, Xining 810008, China; 1707112008@stu.sqxy.edu.cn
* Correspondence: jiawei1212@qhnu.edu.cn
† These authors contributed equally to this work.

Abstract: In recent years, China's economy has experienced rapid development, and its cities have undergone rapid expansion; however, the development of cities in the northwest region has been relatively slow due to various geographical and economic constraints. Studying the urban expansion in these regions is of significant importance for regional planning and development. This study selected the provincial capitals of five underdeveloped provinces in northwestern China as the research sample and used Landsat TM/OLI remote-sensing imagery as the primary data, supplemented by Digital Elevation Model (DEM), meteorological, and socio-economic data, the study extracted urban impervious surfaces using the ENDISI and MNDWI indices. It analyzed the spatial and temporal characteristics of urban impervious surfaces from 1990 to 2020 using indicators such as urban expansion intensity, compactness and fractal dimension, centroid migration, and standard deviation ellipse. Furthermore, the study quantified the influencing factors using Geodetectors. The findings reveal the following: (1) From 1990 to 2020, impervious surfaces in the five cities continued to expand, with Xi'an experiencing the largest expansion area at 549.94 km^2 and Xining the smallest at only 132.83 km^2, with an expansion intensity of merely 2.99%. However, significant disparities existed in expansion intensity and area across different periods. (2) Overall, the compactness of the cities decreased by 47.6% while the overall fractal dimension increased by 2.85%, indicating a trend towards more dispersed and complex urban forms. (3) Expansion directions varied among the cities, with Xi'an and Urumqi expanding towards the northwest, Lanzhou towards the north, Yinchuan primarily towards the east, and Xining mainly towards the west. (4) Economic, demographic, and investment factors were identified as the primary influencers of urban expansion, exhibiting changes over different periods. Analyzing the similarities and differences in city development can offer valuable insights into urban construction and sustainable development in underdeveloped areas.

Keywords: impervious surfaces; urban agglomeration expansion; ENDISI; geodetector; underdeveloped regions

Citation: Feng, Y.; Ma, Y.; Jia, W.; Shu, S.; Li, H.; Hu, X. Spatial and Temporal Changes and Influencing Factors of Capital Cities in Five Provinces of the Underdeveloped Regions of Northwest China. *ISPRS Int. J. Geo-Inf.* **2024**, *13*, 215. https://doi.org/10.3390/ijgi13060215

Academic Editor: Wolfgang Kainz

Received: 24 April 2024
Revised: 5 June 2024
Accepted: 18 June 2024
Published: 19 June 2024

1. Introduction

According to the World Cities Report, *2022: Envisioning the Urban Future*, global urbanization is growing rapidly at an unprecedented rate, with the proportion of the population in urban areas predicted to grow to 68% by 2050 [1]. Rapidly expanding urbanization causes damage to water resources and biodiversity, accelerated carbon dioxide emissions, and reduced energy use efficiency [2–5]. One of the distinctive features of urbanization is the gradual replacement of natural surface landscapes by impervious

surfaces (ISs), which are mainly artificial [6]. These mainly include hard roads, commercial areas, residential areas, and rooftops of buildings in development zones [7]. Existing studies show an increasing trend towards ISs all over the world, with an average increase of about eight times the average loss of tree cover [8]. Therefore, analyzing trends in the expansion of urban ISs is critical for environmental and sustainable development.

Extensive research has been conducted on the impervious surfaces in urban expansion. The earliest studies utilizing classification methods to extract impervious surfaces and apply them to urban expansion focused primarily on using optical and SAR remote sensing data, with classification methods such as spectral mixture analysis, decision tree modeling, and support vector machines [9–11]. When the research scale is expanded to the national or even global scale, the remote sensing image data involved often becomes immense, resulting in substantial computational demands. To address this issue, scholars have proposed using Google Earth Engine combined with multisource and multi-temporal remote sensing data to construct a global impervious surface area dataset [12]. These datasets often span several decades and integrate multiple classification methods, significantly reducing the workload for researchers conducting large-scale urban expansion studies [13,14]. Moreover, using various urban indices to extract impervious surfaces is also an effective approach. Indices such as the Normalized Difference Impervious Surface Index (NDISI), Enhanced Built-Up and Bareness Index (EBBI), and Normalized Difference Built-up Index (NDBI) require minimal preprocessing and are user-friendly, thereby improving the efficiency of impervious surface mapping [15–18]. Utilizing impervious surfaces for urban expansion research is an effective method.

When analyzing the expansion patterns and driving forces of urbanization, studies in different regions and at different scales around the world show diverse conclusions. In terms of urban expansion patterns and morphological changes, Cairo in North Africa and Bangkok in Southeast Asia have relatively low urban compactness and relatively dispersed urban forms [19,20]; in North America, the urban form of the United States is mainly scattered and expanded, with typical cities being Raleigh, Washington, and Houston. The urban form in Europe and China is dominated by central compact shapes, and most cities are developing in the direction of compact shapes and mixed functions, such as Vienna, Austria, and Changzhou, China [21]. As for the driving factors of urban expansion, in highly urbanized areas such as Romania in Europe and Beijing and Shanghai in Asia, socio-economic factors and geographical location affect the development of investment, trade, and tourism, which is accompanied by increasing demand for accommodation, infrastructure, and transportation. The process of urbanization is accelerating [22–24]. In tertiary regions such as the Tibetan Plateau, Pamir, and Hindu Kush, urban expansion is primarily driven by population growth, and topographic elevation limits urban expansion. The construction of streets and roads promotes urbanization [25]. In the spatial and temporal evolution of urban land at different scales, economic factors are dominant at the provincial level, whereas population factors are most significant at the county level, and economic, population, and traffic factors all play an important role at the prefecture-level [26]. In summary, global urbanization presents diverse expansion patterns and diversified drivers, influenced by geographical regions and different scales, and these complexities make urban research richer and more challenging.

To study urban expansion in underdeveloped regions, researchers have examined the population and political policies of these areas, suggesting a close relationship between urbanization, population growth, and political dynamics [27–29]. In regions like Bamako in West Africa, Cairo in North Africa, Nairobi in East Africa, central Myanmar, and southern Vietnam in Southeast Asia, urban expansion often comes at the cost of agricultural land and encroachment on forests and natural landscapes [30–32]. In some underdeveloped areas of China, such as Nanchang, urban planning policies play a central role in driving urban expansion, with physical geography exerting comparatively less influence [33]. The international definition of an underdeveloped region encompasses multiple dimensions, with the United Nations Development Program using life expectancy, education, and per

capita income as indicators for assessing the Human Development Index (HDI) [34]. In 1990, China's HDI was 0.449, indicating a low level of overall human development. Subsequently, China's HDI rose to 0.588, 0.699, and 0.761 in 2000, 2010, and 2020, respectively, reaching the world average level in 2012 [35–38]. In contrast, despite significant urban land expansion, rapid urbanization, and remarkable economic growth in the five northwestern provinces of China (Shaanxi, Xinjiang, Gansu, Ningxia, and Qinghai), the gap with other regions of China continues to widen [39,40]. Their average HDI increased from 0.358 in 1990 to 0.704 in 2020, which was generally lower than the national average, categorizing them as underdeveloped regions. However, there is a dearth of research on the expansion patterns of these provincial capitals, particularly in comparing their divergent models and influencing factors.

Therefore, this study selected the underdeveloped provincial capital cities (Xi'an, Urumqi, Lanzhou, Yinchuan, and Xining) in the five provinces of northwestern China as the study sample. It used Landsat TM/OLI image data as the primary data source, combined with DEM, meteorological, and socio-economic data. Urban spatial morphology indices, center of gravity migration, and standard deviation ellipse models were employed to analyze the similarities and differences in urban impervious surface expansion patterns and change trends in the five capital cities of the underdeveloped regions of China from 1990 to 2020. Meanwhile, the influencing factors of urban expansion in different periods and cities were analyzed by considering socio-economic elements, natural geographic elements, and policy documents. The aim is to study the spatiotemporal characteristics and influencing factors of urban expansion in the underdeveloped cities of the five northwestern provinces of China, providing insights for related research in underdeveloped areas and offering scientific references for urban planning, construction, and sustainable development.

2. Research Area and Data Introduction

2.1. Overview of the Study Area

The Northwest Five Provinces are situated in northwestern China, encompassing Shaanxi Province, Xinjiang Uygur Autonomous Region, Gansu Province, Ningxia Hui Autonomous Region, and Qinghai Province, which lie between 31°32′ and 49°10′ N and 73°15′–111°15′ E (Figure 1). These provinces are predominantly inland, situated mainly on the Loess Plateau, the Tibetan Plateau, and the Tarim Basin, and are characterized by plateaus, mountains, and Gobi desert landscapes. The topography is intricate, precipitation levels are low, and the climate tends to be arid overall. Although the total land area of the five northwestern provinces accounts for 32% of the country's landmass, their combined GDP is 7039.53 billion yuan, representing only 5.87% of the national total. The population of approximately 106 million inhabitants in these provinces constitutes 7.35% of China's total population [41]. Within these provinces, each capital city holds the highest GDP share: Xi'an contributes 35% to its province's GDP, Urumqi accounts for 22%, Lanzhou for 29.85%, Yinchuan for 50%, and Xining for 45.55%. These five provincial capital cities offer a representative basis for investigating urban expansion in less developed areas.

2.2. Data Sources and Preprocessing

The remote-sensing image data used in this paper included 1990, 2000, 2010, and 2020 Landsat TM/OLI data with a spatial resolution of 30 m; the projection was the Universal Transverse Mercator (UTM) projection (Appendix A). The DEM data adopted the SRTM1 (1 arc-second) data set in the region, with a spatial resolution of 30 m. Pre-processing of Landsat images was carried out in the ENVI 5.3 and mainly included radiometric calibration, atmospheric correction, and geometric correction. These data were obtained from USGS [42]. Socio-economic statistics were obtained from the Statistical Yearbook of the Five Northwest Provinces [41]. Precipitation and temperature data were obtained from the ERA5-Land dataset released by the European Union and organizations such as the European Centre for Medium-Range Weather Forecasts [43]. The raw data were month-by-month average precipitation/temperature raster data; year-by-year average pre-

cipitation/temperature raster data were obtained by calculating the average of 12-month average precipitation/temperature using the raster calculation tool. Using these data, the raster values within each municipality were averaged to obtain year-by-year average precipitation (annual average of daily precipitation in that year, in units of m) and year-by-year average air temperature (in units of °C) for each municipality. The average was processed to obtain yearly average precipitation (the annual average of daily precipitation for the year in m) and yearly average air temperature (in degrees Celsius) for each municipality. Elevation and average slope data were calculated for each city with the help of the ArcGIS 10.5.

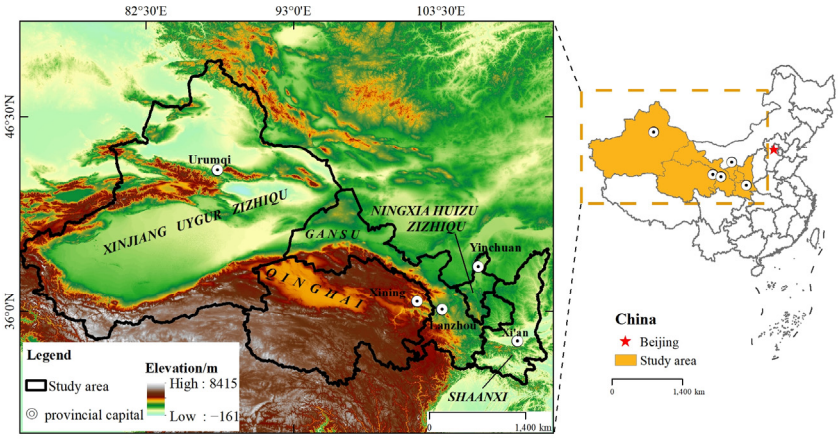

Figure 1. Study area.

3. Methods

Firstly, the Enhanced Normalized Difference Impervious Surface Index (ENDISI) and the Modified Normalized Difference Water Index (MNDWI) were used to extract the impervious surface of the provincial capital cities of the five northwestern provinces for the years 1990, 2000, 2010, and 2020. Subsequently, the spatial and temporal dynamic changes and the morphological evolution characteristics of urban expansion in the study area were analyzed. This involved comparing the expansion rates, intensities, compactness, and fractal dimensions of impervious surfaces across different cities and periods, as well as examining the trajectories of center of gravity migration and standard ellipse differences. Finally, the influencing factors of spatial and temporal dynamics in different cities were analyzed using Geodetector. A technical block diagram of the procedure is illustrated in Figure 2.

3.1. Urban IS Extraction Methods

The Enhanced Normalized Difference Impervious Surfaces Index (*ENDISI*) was proposed on the basis of previous research results. It can effectively eliminate the influence of dry land, bare rock, and bare soil on IS extraction so that water-impervious and water-permeable surfaces can be more effectively separated and extracted [44]. Because part of the study area contains water, when *ENDISI* was used to extract water-impervious surfaces in the study area, the Modified Normalized Difference Water Index (*MNDWI*) was used to mask water [45]. *ENDISI* and *MDNWI* can be calculated by Equations (1) and (2):

$$ENDISI = \frac{\frac{(2B_{Blue}+B_{SWIR_2})}{2} - \frac{(B_{Red}+B_{NIR}+B_{SWIR_1})}{3}}{\frac{(2B_{Blue}+B_{SWIR_2})}{2} + \frac{(B_{Red}+B_{NIR}+B_{SWIR_1})}{3}} \quad (1)$$

$$MNDWI = \frac{B_{Green} - B_{SWIR_1}}{B_{Green} + B_{SWIR_1}} \quad (2)$$

where B_{Blue}, B_{Green}, B_{Red}, B_{NIR}, B_{SWIR_1}, B_{SWIR_2} represent the surface reflectance values of the blue, green, and red light bands, the near-infrared band, and the first and second short-wave infrared bands, respectively.

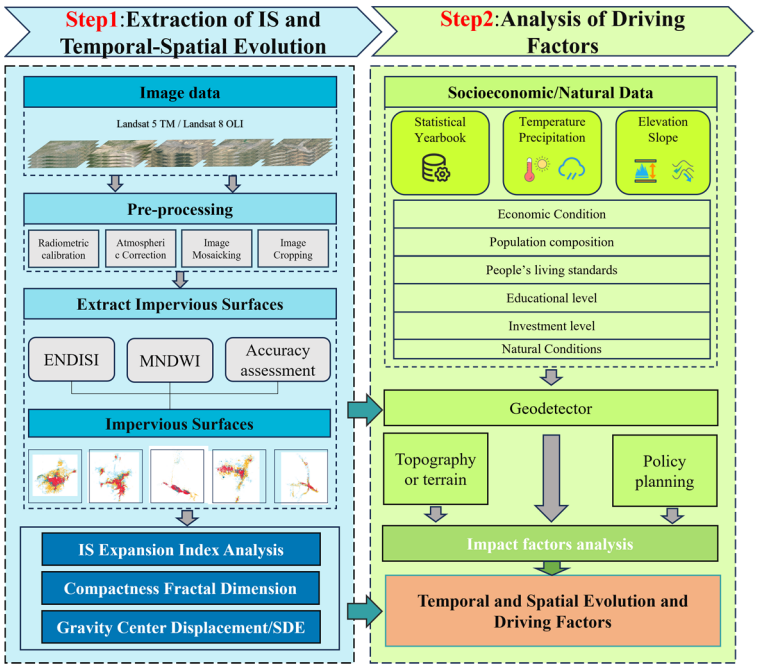

Figure 2. Technical block diagram.

3.2. Verification of Extraction Accuracy of Urban ISs

The reference data for accuracy validation used Google Earth historical contemporaneous high-resolution images and field validation data. In ArcGIS10.5, 200 random sample points were generated, and because the image contents for 1990 and 2000 were incomplete, the ISs of Xining City in 2010 and 2020 were compared with Google Earth high-resolution images from the same period and were verified by human–computer interaction. ISs in 2020 were verified in the field.

The accuracy of the extraction was verified using historical high-resolution imagery from Google Earth and field verification data. Due to the incomplete Google Earth high-resolution imagery for 1990 and 2000, we primarily selected Xining for verification and validated the impervious surface extraction results for 2010 and 2020. The verification data for 2010 were generated through random sample points in ArcGIS 10.5, while the verification data for 2020 included both random sample points generated in ArcGIS 10.5 and field verification sample points. The random sample points generated in ArcGIS 10.5 were compared with historical high-resolution imagery data in Google Earth on a point-by-point basis. The field verification sample points were compared through on-site field verification. The accuracy of the extraction was calculated by determining the proportion of correctly extracted impervious surface sample points to the total number of selected impervious surface sample points. The calculation formula is as follows Equation (3):

$$A = \frac{C}{T} \times 100\% \tag{3}$$

where A represents the extraction accuracy, C is the number of correctly extracted impervious surface sample points, and T is the total number of selected impervious surface sample points.

3.3. Urban IS Expansion Intensity Index

The IS expansion strength index I was used to reflect the ratio of the annual average IS expansion area over a time period to the IS area of the base year to assess the strength of IS expansion in different regions and at different stages. It was computed using Equation (4):

$$I = \left(\frac{S_B - S_A}{TS_A} \right) \times 100\% \tag{4}$$

where S_B is the urban IS area in the year of interest, S_A is the urban IS area in the base year, and T is the time interval in years.

3.4. Compactness Index and Fractal Dimension

The compactness index (P) is an important index used to measure the degree of spatial aggregation of landscape patches. The smaller the P is, the more discrete the distribution of IS patches within the city. The larger the P is, the more aggregated the IS patches, the more compact the shape, and the less spatial segregation between the patches [46].

Fractal dimension (F) is a mathematical concept used to describe the complexity of boundary shapes and is often applied to the study of IS and urban land-use structures. Theoretically, the fractal dimension range is usually between 1 and 2. When F is less than 1.5, this indicates that the boundary is relatively simple and may reflect regular urban land-use structure; when F is greater than 1.5, this indicates that the boundary is more complex and may be caused by irregular patches or topography. When F is equal to 1.5, this indicates that the boundary is in a state of Brownian motion and that the urban land-use structure may be somewhere between simple and complex [47].

The compactness index (P) and fractal dimension (F) are calculated as Equations (5) and (6):

$$P = \frac{2\sqrt{\pi S}}{C} \tag{5}$$

$$F = \frac{2\ln\left(\frac{C}{4}\right)}{\ln S} \tag{6}$$

where S and C are the area and perimeter of the impervious surfaces in the city.

3.5. Center of Gravity Migration and Standard Deviation Ellipses

Center of gravity migration trajectory analysis is usually based on the movement direction of the weighted average center of geographic elements (also known as the center of mass or center of gravity). It can be used to characterize the expansion trend of ISs in a city because it can reveal the migration law of the center of mass of the ISs in the process of urban expansion and can effectively reflect the dynamic process and spatial change of the city's development. This can help us understand the adjustment and evolution of the urban spatial structure. The standard deviational ellipse (SDE) is a tool in spatial statistical analysis that can quantitatively describe the directionality of the spatial distribution and the spatial structural characteristics of ISs based on the spatial location and structure of geographic elements by calculating parameters such as the long axis, the short axis, and the azimuthal angle of the ellipse [48].

The spatial center of gravity of the ISs can be calculated using Equation (7):

$$\begin{cases} X_t = \frac{\sum_{i=1}^{n}(W_i x_i)}{\sum_{i=1}^{n} W_i} \\ Y_t = \frac{\sum_{i=1}^{n}(W_i y_i)}{\sum_{i=1}^{n} W_i} \end{cases} \tag{7}$$

and the standard deviation ellipse azimuth can be calculated using Equation (8):

$$tan\theta = \frac{(\sum_{i=1}^{n} W_i^2 \widetilde{x}_i^2 - \sum_{i=1}^{n} W_i^2 \widetilde{y}_i^2) + \sqrt{(\sum_{i=1}^{n} W_i^2 \widetilde{x}_i^2 - \sum_{i=1}^{n} W_i^2 \widetilde{y}_i^2)^2 + 4\sum_{i=1}^{n} W_i^2 \widetilde{x}_i^2 \widetilde{y}_i^2}}{2\sum_{i=1}^{n} W_i^2 \widetilde{x}_i \widetilde{y}_i} \quad (8)$$

The long and short axes are calculated using Equation (9):

$$\begin{cases} \sigma_x = \sqrt{\frac{\sum_{i=1}^{n} (w_i \widetilde{x}_i cos\theta - w_i \widetilde{y}_i sin\theta)^2}{\sum_{i=1}^{n} w_i^2}} \\ \sigma_y = \sqrt{\frac{\sum_{i=1}^{n} (w_i \widetilde{x}_i sin\theta - w_i \widetilde{y}_i cos\theta)^2}{\sum_{i=1}^{n} w_i^2}} \end{cases} \quad (9)$$

In Equations (6)–(8), X_t and Y_t are the latitude and longitude of the center of gravity in year t; W_i is the area of the IS within the i-th cell; x_i and y_i denote the longitude and latitude of the geometric center within the i-th cell, respectively. θ is the ellipse azimuth angle; $\widetilde{x}_i$ and $\widetilde{y}_i$ are the longitude and latitude of the deviation of each IS patch from the ellipse's center of gravity; σ_x and σ_y are the standard deviation of the ellipse in the x- and y-directions. The long and short axes of the standard deviation ellipse can be used to reflect the degree of dispersion of the IS in the x- and y-directions.

3.6. Driver Indicators and Geodetector

Currently, studies on factors influencing urban expansion utilize a variety of indicators. Typically, these indicators include industrial structure and GDP, which drive the transformation of urban expansion [49]. Factors such as population growth, natural environment and locational constraints, and increasing income levels among residents also contribute to increased demands for residential, transportation, and public facilities, necessitating the use of more land resources and expansion of urban areas to meet these needs [50–52]. Furthermore, rising levels of investment and improvements in education also lead cities to expand into larger spaces [53–55]. Based on a comprehensive analysis of these urban expansion studies and considering our study area, we have selected six major categories (economic, population, living standards, education level, investment level, and natural factors) comprising 18 indicators (Table 1) to quantitatively analyze the impact of these factors on impervious surface expansion using geographic detectors. Geodetector is a set of statistical methods for detecting spatial heterogeneity and revealing the driving forces behind it [56]. The Geodetector model is calculated using Equation (10):

$$q = 1 - \frac{\sum_{h=1}^{L} N_h \sigma_h^2}{N\sigma^2} \quad (10)$$

where q is the explanatory power of the driver of IS expansion in the study area, N is the sample size of the study area, σ^2 is the variance, and q ranges from 0 to 1. The larger the value, the greater will be the explanatory power of the factor for IS expansion.

Table 1. The influencing factors of urban expansion are selected.

Variable Category	Variable Description
Independent variables	Impervious Surfaces Area (km^2)/(Y)
Economic Condition/(X1)	Regional Gross Domestic Product (10,000 yuan)/(X11) Value added of the secondary industry (million yuan)/(X12) Value added of the tertiary industry (10,000 yuan)/(X13)

Table 1. *Cont.*

Variable Category	Variable Description
Population/(X2)	Registered population (10,000 people)/(X21) Number of employees in the secondary industry (10,000 people)/(X22) Number of employees in the tertiary industry (10,000 people)/(X23)
Living standards/(X3)	Total wages of employees on duty (10,000 yuan)/(X31) Average salary of employees (yuan)/(X32) Number of doctors (person)/(X33)
Educational level/(X4)	Number of full-time teachers in ordinary middle schools (person)/(X41) Number of full-time primary school teachers (person)/(X42) Number of full-time teachers in ordinary higher education institutions (person)/(X43)
Investment level/(X5)	Fixed Assets Investment (10,000 yuan)/(X51) Completed investment in real estate development (10,000 yuan)/(X52)
Natural condition/(X6)	Average annual daily precipitation (m)/(X61) Annual average temperature (°)/(X62) Elevation (m)/(X62) Average slope (°)/(X63)

4. Results and Analysis

4.1. Accuracy Assessment

This study evaluated the accuracy using Xining as the subject. In 2010, out of 200 selected impervious surface samples in Xining, 165 were correctly extracted through comparison with Google Earth imagery, resulting in an overall accuracy of 82.5% (Figure 3a). In 2020, out of 200 selected impervious surface samples in Xining, 175 were correctly extracted through comparison with Google Earth imagery, resulting in an overall accuracy of 87.5%. In 2023, through field validation, out of 83 selected impervious surface samples in Xining, 69 were correctly extracted, achieving an overall accuracy of 83.13%, meeting the requirements of this study (Figure 3b).

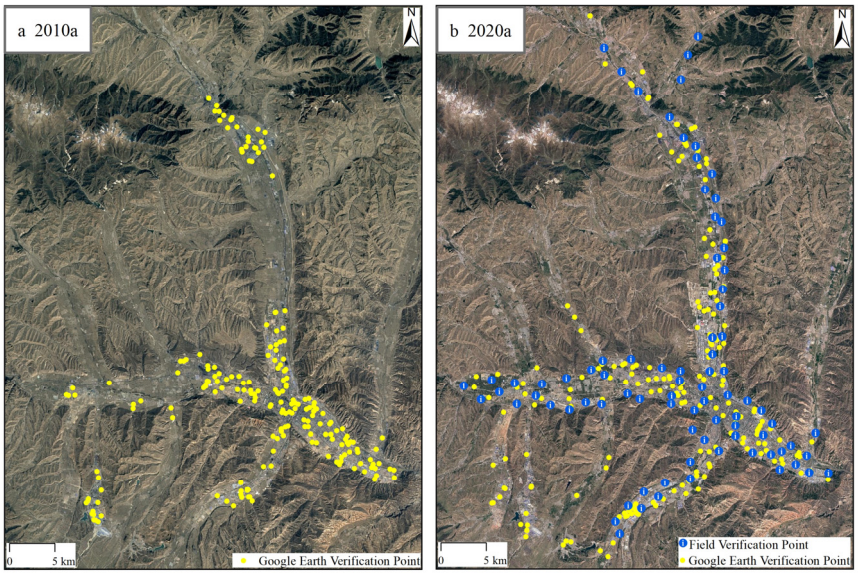

Figure 3. Google Earth verification points and field verification points distribution; (**a**) the Google Earth verification points distribution of Xining in 2010, (**b**) the Google Earth verification points distribution of Xining in 2020.

4.2. Spatial and Temporal Characteristics of IS Expansion in the Capital Cities of the Five Northwestern Provinces

In 1990–2020, the expansion of ISs in the capital cities of the five northwestern provinces is shown in Figure 4. Information on the expansion area (EA) and expansion intensity (EI) of urban ISs appears in Table 2.

Table 2. Area and intensity of IS expansion in capital cities of five northwestern provinces.

City	Year							
	1990–2000		2000–2010		2010–2020		1990–2020	
	EA	EI	EA	EI	EA	EI	Total EA	Total EI
Xi'an	89.37	4.90%	326.65	12.01%	133.92	2.24%	549.94	10.04%
Urumqi	84.53	2.94%	143.27	5.98%	218.70	5.71%	446.5	7.50%
Lanzhou	38.76	2.62%	57.64	3.09%	36.43	1.49%	132.83	2.99%
Yinchuan	21.75	4.22%	85.47	11.67%	52.46	3.30%	159.68	10.33%
Xining	15.49	3.47%	72.74	12.09%	87.71	6.60%	175.94	13.13%

Overall, from 1990 to 2020, the expansion areas of the capital cities of the five northwestern provinces all became larger, among which Xi'an had the largest expansion area, and by 2020, the overall expansion area reached 549.94 km^2 (Figure 4(a4)). The Urumqi total expansion area was in second place, at 446.5 km^2 (Figure 4(b4)). The pattern of IS expansion varied significantly but spatially showed a ring-like expansion trend. The expansion area of the other three cities was relatively small, less than 200 km^2 and the spatial change represented mainly a shift of the urban area in other directions, showing strip- and cross-shaped expansion trends. In terms of expansion intensity, Xining, Yinchuan, and Xi'an all had an overall expansion intensity greater than 10%, of which Xining had the highest overall expansion intensity (13.13%) and Urumqi was in the middle expansion intensity range, at 7.5%. Lanzhou, on the other hand, had the lowest total expansion intensity during the 30-year period, at only 2.99%.

From the perspective of each time period, the expansion trend of each city showed a "small-large-small" trend. Between 1990 and 2000, Xi'an and Urumqi had the largest expansion areas, reaching 89.37 km^2 and 84.53 km^2 respectively, and the ISs became more compact, with Xi'an tending to extend into the western part of the city, and Urumqi becoming more compact within the original urban area (Figure 4(a2,b2)). Lanzhou and Yinchuan had medium-sized expansion areas, and Xining had the smallest expansion area, at only 15.49 km^2. Their urban morphology did not change significantly, and they mainly infilled on the basis of their original urban areas, with weak overall expansion. Xi'an and Yinchuan had the highest intensity of expansion during this period, at 4.9% and 4.22%, respectively. From 2000 to 2010, the expansion area and intensity of the five cities further increased. Xi'an still led the way with the largest expansion area (326.65 km^2) and highest expansion intensity (12.01%), with a more complex urban morphology and significant expansion to the north and southwest (Figure 4(a3)). Xining and Yinchuan had smaller expansion areas, but higher expansion intensities, reaching 11.67% and 12.09%, respectively, and Yinchuan showed a very obvious urban infill in the north-south direction, connecting the urban area from north to south and expanding coverage of the whole city (Figure 4(d3)). Xining was more completely filled up in the northern part of the city, and therefore new urban areas expanded in the western and southern parts. Lanzhou and Urumqi also continued to grow in terms of urban expansion area and intensity, with Urumqi's expansion area reaching 143.27 km^2 and the construction of new urban areas in the northwest becoming more complete. Lanzhou's expansion area also grew to 57.64 km^2, with piecemeal expansions mainly in the east and north, but with lower intensity in both cities (Table 2).

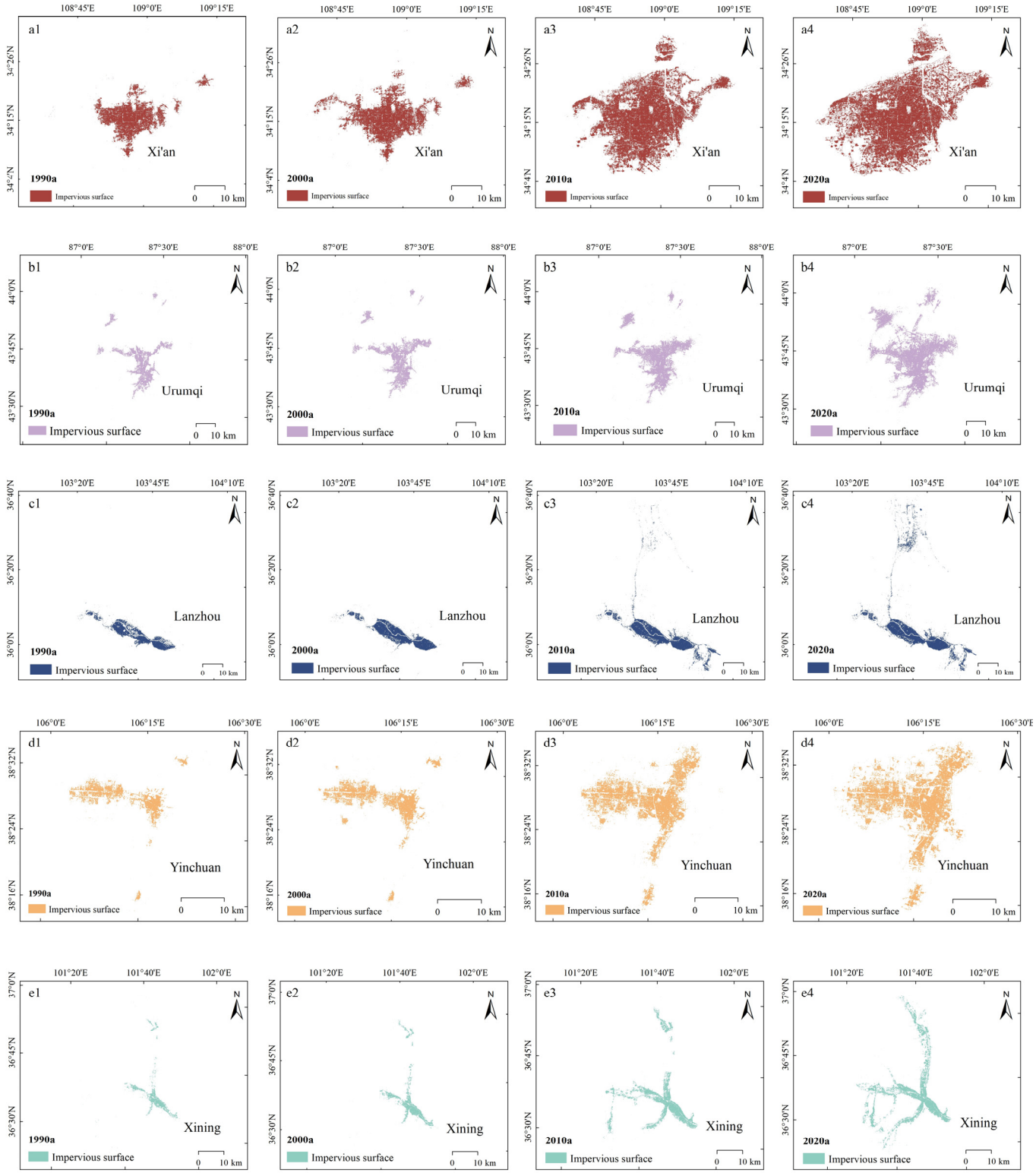

Figure 4. IS expansion in capital cities of five northwestern provinces, 1990–2020; (**a1**–**a4**) IS of Xi'an in 1990, 2000, 2010 and 2020, (**b1**–**b4**) IS of Urumqi in 1990, 2000, 2010 and 2020, (**c1**–**c4**) IS of Lanzhou in 1990, 2000, 2010 and 2020, (**d1**–**d4**) IS of Yinchuan in 1990, 2000, 2010 and 2020, (**e1**–**e4**) IS of Xining in 1990, 2000, 2010 and 2020.

From 2010 to 2020, except for the expansion areas of Urumqi and Xining that were still growing, the expansion areas of the remaining three cities have decreased considerably (Table 2). Urumqi's expansion area grew and broke through to 218.7 km^2, which was

the largest expansion area among the five cities in this period, with a larger expansion range of the main urban area and further construction in the new northern area. Xining expanded the IS area to 87.71 km^2 in this period, surpassing Lanzhou and Yinchuan and connecting the northern part of the city to the main urban area, with the urban area taking on the shape of a cross (Figure 4(e4)). Although the intensity of urban expansion in Xi'an declined, the area of expansion was still more than 100 km^2, and the urban area crossed over to the northeast and southwest based on the original foundation. The expansion area and intensity in Lanzhou and Yinchuan both decreased more in this period than in the previous period. In terms of urban morphology, Lanzhou's northward expansion was the most obvious, and Yinchuan's suburbs further increased coverage of the main urban area through further construction (Figure 4(c4,d4)).

4.3. Morphological Evolution Characteristics of IS Expansion in the Capital Cities of the Five Northwestern Provinces

Based on information on the ISs of the five capital cities in the four periods, the compactness and fractal dimension of each city in different periods have been calculated (Figure 5).

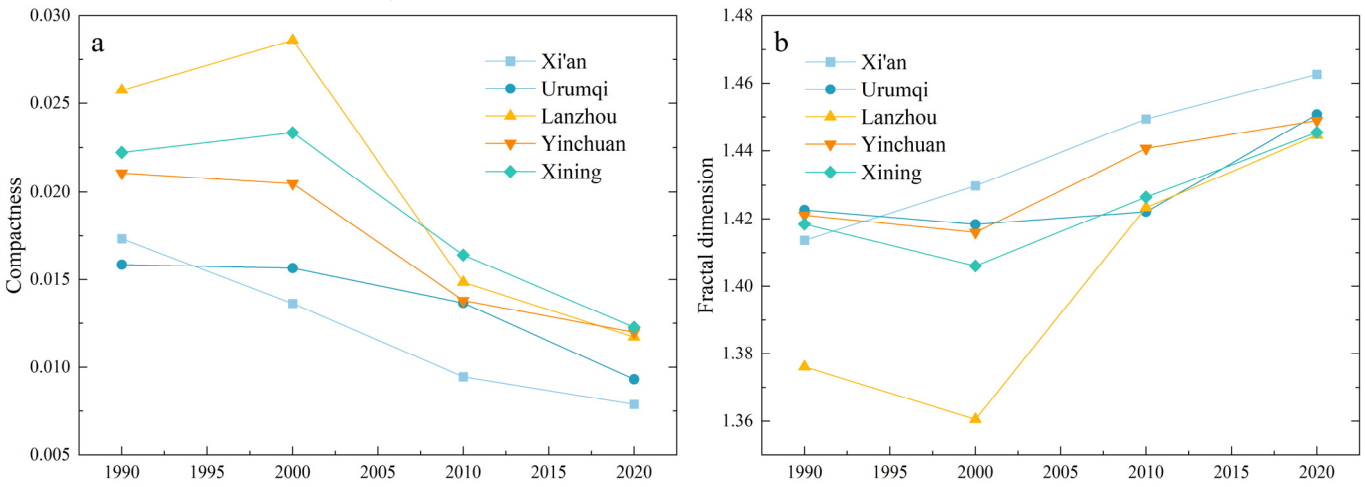

Figure 5. Trends in compactness (**a**) and fractal dimension (**b**) of capital cities in five northwestern provinces.

During the 30 years, the compactness of all five cities exhibited a decreasing trend with a significant rate of decline (Figure 5a). Among them, Lanzhou experienced the highest rate of decline (54.46%), whereas Urumqi showed the lowest rate of decline (41.29%). In terms of periods, from 1990 to 2000, the compactness of Lanzhou and Xining increased by 0.003 and 0.001, indicating a period of intensified land use, with the expansion of these two cities becoming increasingly compact (Figure 5a). However, after 2000, the compactness of each city started to decline sharply. From 2000 to 2010, its rate of decline in the five cities increased significantly. Lanzhou experienced the largest decline, dropping from 0.029 to 0.015, with a rate of decline of 48.28%, whereas Urumqi had the smallest decline, at 12.67%. The other three cities had moderate rates of decline, with Xi'an, Yinchuan, and Xining experiencing rates of decline of 30.74%, 32.58%, and 29.65%, respectively. Since 2010, except for Urumqi, which declined from 0.014 to 0.009 with a rate of decline of 31.89%, the rates of decline of compactness in the other cities began to slow down. Particularly noteworthy was Lanzhou, which exhibited the steepest rate of slowdown, with its rate of decline dropping from 48.28% in the previous period to 20.97%. These changes reflected significant differences in the spatial layout and urban form of the cities over the past three decades. In general, the spatial configuration of ISs in the urban areas of the five cities evolved from a compact form to one that is more dispersed, indicating a transition towards a pattern of loose expansion.

The fractal dimension of each city in 1990–2020 generally showed an increasing trend (Figure 5b), indicating that the urban land use structure generally developed towards complexity. Lanzhou had the strongest growth trend, from 1.376 to 1.445 with a growth rate of 4.98%, which indicated that Lanzhou's urban morphology became more irregular during this period. The fractal dimension of Xi'an grew from 1.414 to 1.463 with a growth rate of 3.47%, making it the city with the most complex boundary among the five cities. The other three cities had a higher base of fractal dimension, with a similar growth rate of approximately 2%. In terms of the time period, only Xi'an's fractal dimension grew from 1990 to 2000, and this trend continued in the later period as well. Urumqi and Yinchuan had smaller decreases, from 1.423 and 1.421 to 1.418 and 1.416; Lanzhou itself had the smallest fractal dimension among the five cities, only 1.376, with a simpler shape, and Lanzhou and Xining experienced decreases of 0.016 and 0.012 in this period. From 2000–2010, the fractal dimensions of all five cities started to grow, and this trend also continued in the later period. The urban structure shifted to more complex development, with Lanzhou City growing the fastest; its fractal dimension grew from 1.36 to 1.423, with a growth rate of 4.63%. The growth rate of Urumqi's fractal dimension was low, at only 0.2%. Xi'an, Yinchuan, and Xining had growth curves that tended to be parallel, and the growth rates were also similar, with fractal dimensions of 1.449, 1.44, and 1.426, respectively. From 2010 to 2020, Urumqi's fractal dimension continued to increase to 1.45, with a growth rate of 2%; growth in all other cities began to slow down, especially in Lanzhou, where the slowdown was most pronounced, with the growth rate dropping to 1.49%. However, in this period, the fractal dimensions of all five cities reached their historical maxima. These data suggested that the shape of the IS boundary in these cities became more complex and irregular over time.

4.4. Evolution of IS Expansion Direction and Spatial Shift of Center of Gravity in the Capital Cities of the Five Northwestern Provinces

Using the ArcMap 10.5 software, migration information for the SDA parameter and the center of gravity coordinates for the capital cities of the five northwestern provinces were obtained through the directional distribution tool (Figure 6); the statistical results are presented in Table 3.

Table 3. SDE parameters for capital cities in five northwestern provinces.

City	Year	Barycentric Coordinates	Semi-Major Axis	Semi-Minor Axis	Oblateness
Xi'an	1990	108.981° E, 34.276° N	15.485	8.141	0.474
	2000	108.926° E, 34.286° N	18.626	9.312	0.5
	2010	108.933° E, 34.291° N	18.571	13.05	0.297
	2020	108.916° E, 34.302° N	22.315	12.755	0.428
Urumqi	1990	87.524° E, 43.882° N	18.917	14.137	0.253
	2000	87.519° E, 43.869° N	19.002	13.133	0.309
	2010	87.547° E, 43.903° N	19.233	15.699	0.184
	2020	87.506° E, 43.913° N	21.945	16.325	0.256
Lanzhou	1990	103.668° E, 36.113° N	21.631	5.674	0.738
	2000	103.630° E, 36.111° N	21.239	5.772	0.728
	2010	103.719° E, 36.239° N	35.693	18.473	0.482
	2020	103.705° E, 36.317° N	38.566	17.261	0.552
Yinchuan	1990	106.195° E, 38.468° N	9.869	7.31	0.259
	2000	106.120° E, 38.463° N	10.45	9.186	0.121
	2010	106.222° E, 38.468° N	11.974	10.138	0.153
	2020	106.222° E, 38.470° N	12.322	11.204	0.091
Xining	1990	101.728° E, 36.692° N	16.826	8.573	0.49
	2000	101.726° E, 36.710° N	17.729	8.245	0.535
	2010	101.679° E, 36.666° N	18.507	12.381	0.331
	2020	101.650° E, 36.690° N	26.627	12.203	0.542

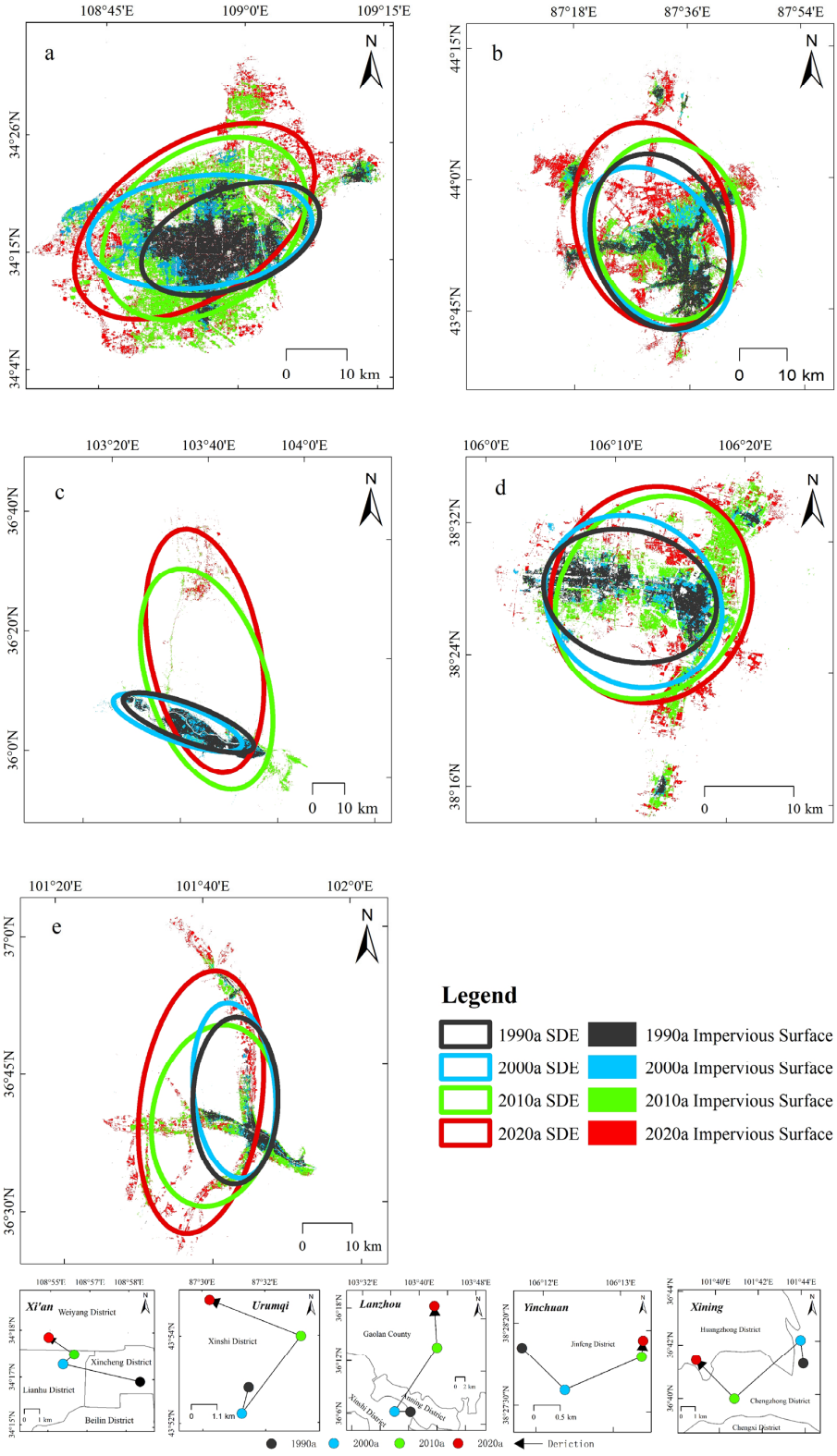

Figure 6. SDE and center of gravity migration trajectories in capital cities of five northwestern provinces; (**a**) SDE changes in Xian, (**b**) SDE changes in Urumqi, (**c**) SDE changes in Lanzhou, (**d**) SDE changes in Yinchuan, (**e**) SDE changes in Xining.

The cities' urban centers of gravity migrated considerably during the 30 years, with Xi'an and Urumqi expanding mainly in a northwesterly direction, Lanzhou and Xining expanding mainly in a north-south direction, and Yinchuan expanding mainly in an east-

west direction. Overall, the urban centers of gravity of Xi'an and Urumqi shifted northward by 0.026° and 0.031° and westward by 0.065° and 0.018°, respectively, between 1990 and 2020, with the cities expanding northwestward. The oblateness, although decreasing after 2000, continued to grow after 2010, with the urban form developing from compact to flat. Lanzhou had the largest northward shift in its center of gravity, with a northward shift of 0.204°; the long semiaxis grew significantly from 21.631 km to 38.566 km, the oblateness decreased by 0.176 after 2000, and the east-west directionality of the city's development diminished and slowly shifted to the north and south (Figure 6c). Yinchuan's urban center of gravity migration was less, its oblateness was very small (0.091), and the standard deviation ellipse tended to become more rounded, indicating that the multi-directionality of urban expansion in the north-south and easterly direction was more complete (Figure 6d). Xining's urban center of gravity migrated westward by 0.078°, its oblateness decreased by 0.159 during 1990–2010, and the expansion of the city was more directional, However, by 2020, the semi-major axis of Xining surged to 26.627 km and the oblateness increased to 0.542, indicating that the city had become more integrated in its spatial pattern of development (Figure 6e).

In terms of time segments, Xi'an experienced the most significant migration of its urban center from 1990 to 2000, with a subsequent decrease in migration amplitude post-2000, settling in the Weiyang District (Figure 6). Urumqi witnessed considerable migration during the period from 2000 to 2020, with migration parameters remaining similar. Notably, between 2000 and 2010, its center of gravity mainly shifted northeastward, transitioning to a northwestward migration after 2010, yet its urban center consistently remained in the new urban area. Lanzhou and Xining exhibited the largest migration amplitudes from 2000 to 2010, with Lanzhou predominantly moving northward and Xining southwestward. Post-2010, Lanzhou's northward expansion persisted, but Xining shifted northwestward. Yinchuan experienced the greatest migration volume from 1990 to 2010, but declined post-2010. Despite briefly shifting southward, its migration primarily resumed eastward, with minimal migration post-2010.

4.5. Analysis of Factors Influencing IS Expansion in the Capital Cities of the Five Northwestern Provinces

Based on the selected six primary categories and 18 secondary categories of indicators that have a greater impact on urban sprawl, the influencing factors of each city in different periods were analyzed using Geodetector; the results are shown in Figure 7.

From 1990 to 2000, the factors as a whole contributed more to the cities of Xi'an, Urumqi, and Lanzhou (Figure 7a,a′). During this period, the indicators with the largest contribution rate in Xi'an were economy and population, which amounted to 0.86 and 0.82, respectively, of which the contribution rate of X23 was the largest, amounting to 0.93. Education level contributed much more to the city of Urumqi than to the other four cities, amounting to 0.67, whereas its contribution to Xi'an was only 0.18. The level of investment contributed the most to Xi'an, with a value of 0.66. This situation is due to the fact that Xi'an has a better educational foundation, but the contribution of the increase in the level of education to the expansion of the city was not as large as the driving energy of investment. The same was true for Lanzhou, which had the smallest contribution to the city's development from education, at only 0.17. For the level of education in Yinchuan and Xining in this period, the main influencing factors were population, living standard, and education level. X32 was the main factor affecting the living standard, with values of 0.83 and 0.89, respectively; the level of investment contributed very little to these two cities in this period, with Yinchuan scoring only 0.1. During this period, the contribution rate of natural factors to the five cities was small, and Xi'an, which had the largest contribution rate of natural factors, only reached 0.3. In Urumqi and Lanzhou, like Xi'an, the contribution rate of natural factors in these three cities is much smaller than that of their economy and population to urban expansion, indicating that the natural environment played no key role in the development of these three cities during this period. It is worth noting that in

Yinchuan and Xining City, the population factor contributed the most to these two cities during this period, while the contribution rate of economic factors was even less than that of natural factors. To a certain extent, this reflects the weak economy of Yinchuan and Xining during this period. The thrust of urban expansion mostly depended on the increase of population, and the economic development had not yet entered the booming period.

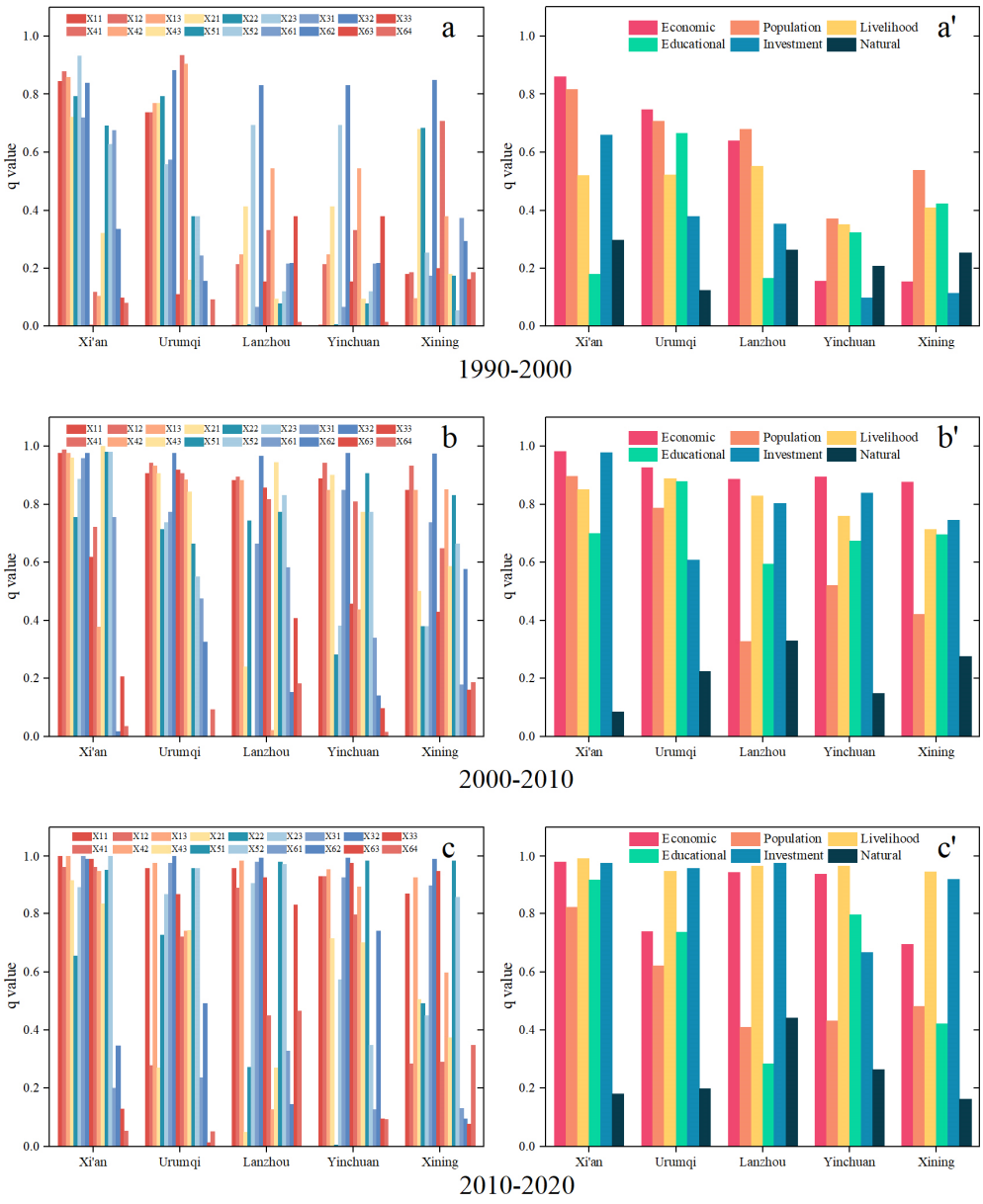

Figure 7. Results of analyzing the factors that influenced the expansion of five provincial capital cities, 1990–2020; (**a**–**c**) the factors influencing the 18 s-level categories; (**a′**–**c′**) the factors influencing the six first-level categories).

From 2000 to 2010, there was a further increase in the contribution of each factor to urban development (Figure 7b,b′). Economic factors saw the most significant growth in Yinchuan and Xining, rising from 0.15 to 0.89 and 0.87, respectively. Conversely, the contribution of population factors declined notably in Lanzhou, dropping from 0.679 to 0.33. Notably, living standards contributed significantly to Yinchuan and Xining during this period, with increases of 0.411 and 0.306, respectively, driven by X31 and X33. X31 surged from 0.06 to 0.84 and 0.73, respectively, whereas X33 climbed from 0.15 and 0.2 to 0.45 and 0.43, indicating the pivotal role of wage levels and health care in urban development. In

Yinchuan, the contribution of the investment level soared from 0.1 to 0.84, primarily due to increases in X51 and X52, showcasing significant achievements in investment attraction and urban housing construction. Moreover, the contribution of education level surged the most in Xi'an and Lanzhou, rising from 0.18 and 0.17 to 0.7 and 0.59, respectively. Notably, the impact of X43 on urban expansion surpassed that of X41 and X42, underlining the role of faculty strength in higher education institutions as a driving force for urban construction. Moreover, the influence of natural factors on cities declined during this period, particularly in Xi'an, which experienced the most significant decline, One of the reasons may be that Xi'an is located in the Guanzhong Plain, with a vast and high-quality land to provide space for urban development. Moreover, the contribution rate of the other five indicators during this period, especially the economy and education, would be ignored to a certain extent. In contrast to Xi'an, the contribution rate of natural factors to Lanzhou's urban expansion increased during this period. It is worth noting that if the contribution rate of natural factors increased in this city, the urban development of this city would be subject to more obvious natural restrictions. Lanzhou encountered certain restrictions during this period, and so did Xining.

From 2010 to 2020, the expansion of urban areas in each city continued to be primarily driven by economic factors, living standards, and investment (Figure 7c,c′). Notably, there was a significant increase in the influence of living standards on urban expansion, which was particularly evident in Xi'an, where the average contribution rate surged from 0.85 in the previous period to 0.99. The contribution rate of population to urban expansion declined in Xi'an, Urumqi, and Yinchuan, suggesting that urban development had reached saturation in terms of population and that the demographic dividend's contribution to urban development was gradually diminishing. Moreover, the contribution of economic development level decreased in Urumqi and Yinchuan, being replaced by an increase in the contribution of investment level, which had a greater impact on Urumqi, Lanzhou, and Xining during this period. In addition, there were changes in the influence of natural factors, with Lanzhou City showing the most obvious response, with the contribution rate of natural factors increasing continuously from 0.33 to 0.44. The contribution of X61 to urban expansion decreased further, and the impacts of X63 and X64 on urban expansion in Lanzhou significantly increased from 0.4 and 0.18 in 2010 to 0.83 and 0.47, respectively. Overall, the development of cities during this period was closely intertwined with living standards, investment attraction, and the natural environment in which they are situated. With the broad growth of the urban economy and the increase of the population, living standards and investment become additional drivers for development within the city. For example, when people seek a better living environment, they may migrate to suburbs with better environmental quality. Corresponding to this, the investment of real estate companies in urban construction continued to increase, and the contribution of real estate development completion investment X14 continued to increase during this period. Similarly, the economic development of cities has led to improvements in urban infrastructure, attracting investment in fixed assets such as factories and industrial parks. These investments are often spatially concentrated in undeveloped areas on the outskirts of the city, which to some extent actively promotes the expansion of the city.

5. Discussion

This study found that the capital cities of the five northwestern provinces continued to expand from 1990 to 2020, which is consistent with previous studies [57]. Urban development varies across cities, regions, and countries and is affected by diverse economic and demographic factors [58]. This study showed the variability in the development of the capital cities of the five northwestern provinces: although all cities had a higher expansion intensity and their urban forms have become more decentralized and complex, each city has migrated differently in the direction of spatial development, and these changes have been influenced by different factors at different times, with each factor having a different magnitude of influence on each city.

5.1. The Effect of Topography on Urban Development

In addition to these influencing factors on urban expansion, topographical factors can also limit the spatial extent of urban development. Xi'an, situated in the Guanzhong Plain, lies less than 10 km south of the Qinling Mountains (Figure 8a). Moreover, the eastern region of Xi'an, which is characterized by the Bailu Plain with higher terrain, imposes constraints on eastward expansion. Consequently, Xi'an's expansion has predominantly occurred westward and northward, leading to the establishment of areas like the Xixian New Area and Jinghe New City.

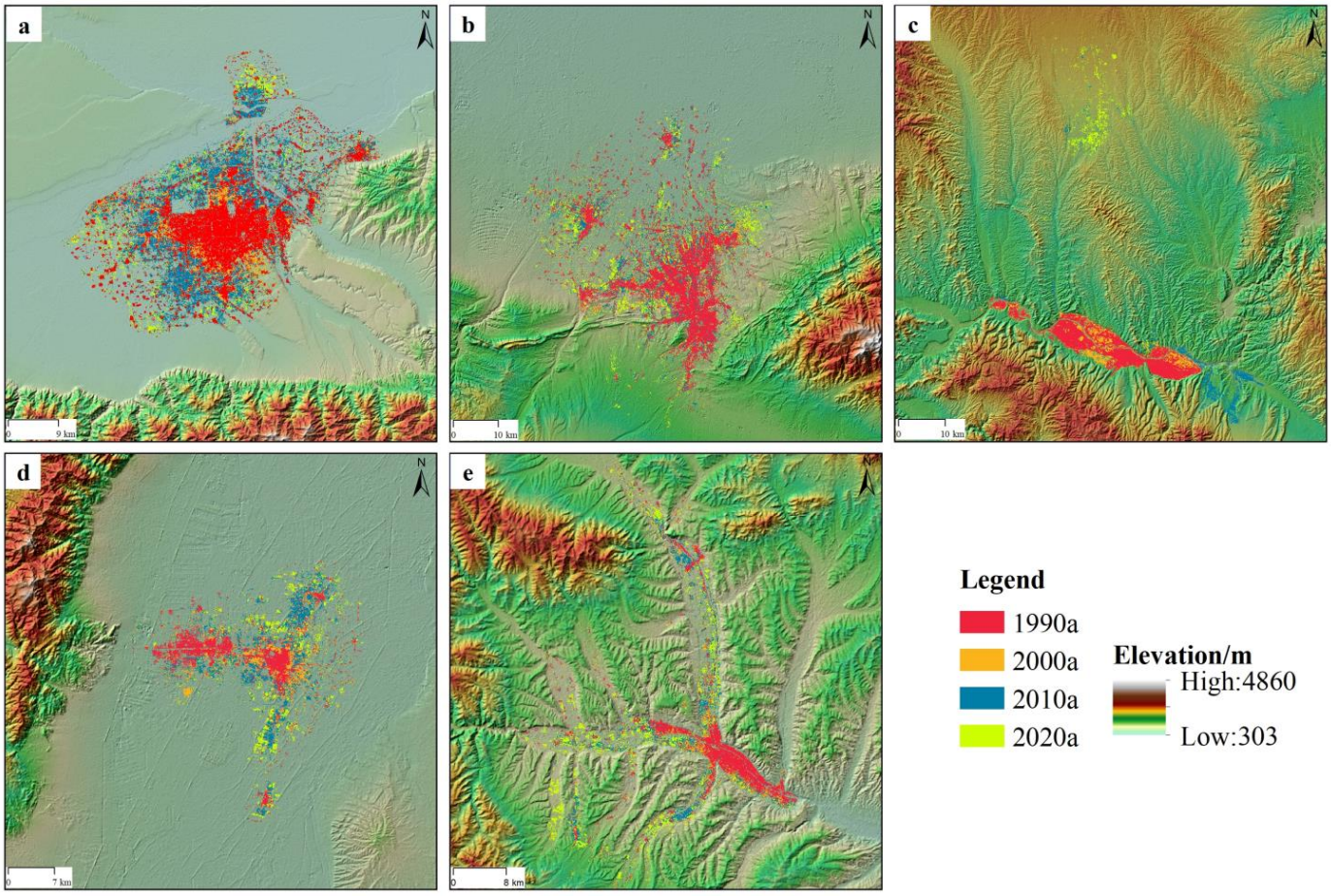

Figure 8. Topographic map of the capital cities of the five northwestern provinces; (**a**) Xi'an, (**b**) Urumqi, (**c**) Lanzhou, (**d**) Yinchuan, (**e**) Xining.

Urumqi, encompassed by mountains on three sides and located in the northern foothills of the Northern Tianshan Mountains, features the Boda Mountains to the east and the Karaza and West Mountains to the west. The northern plains have been the only open and suitable areas for urban construction and development, driving Urumqi's urban expansion over the past three decades (Figure 8b). Lanzhou and Xining, both typical river valley cities, face significant topographical constraints to their expansion. In Lanzhou, where the Yellow River flows through, the surrounding areas are mountainous, with the valley primarily oriented east-west. This geographical layout limits urban construction to the river valley, resulting in constraints on available land for development. Before 2010, Lanzhou's urban shape resembled a "−" type (Figure 8c). Similarly, Xining faces topographical constraints because it is located in the Huangshui Valley, surrounded by mountains and bordered by Haidong in the east (Figure 8e). The city's expansion is limited to the remaining undeveloped valley areas, resulting in a city shape akin to a "+". Conversely, Yinchuan benefits from relatively flat terrain, with the Yellow River passing through and

the Helan Mountains to the west. The urban area primarily occupies the eastern floodplain, offering more open terrain and better conditions for north-south expansion (Figure 8d).

5.2. Differences in the Development of Different Chinese Cities under the Guidance of Policies

Each city has its unique development mode and rapid development period. According to the level of social and economic development and regional development policies, Chinese cities can be divided into four major regions: the eastern coastal region, the northwest region, the central region, and the northeast region. Since 1992, when China established the goal of a socialist market economy system, rapid economic development has promoted urban expansion across the country, especially in the eastern coastal areas such as Shenzhen, Guangzhou, and Shanghai [59–62]. Since 2000, China has continued to develop rapidly, and its economy has further expanded after it acceded to the WTO. At the same time, the state promulgated a series of policies to support the development of the western and central regions, such as the Western development in 2000, the revitalization of the Northeast in 2004, and the rise of the Central region in 2006 [63]. During this period, the economy of the five northwestern provinces grew rapidly, the capital cities in particular attracted a large number of people, and the urban expansion was rapid. The annual growth rate of expansion gradually increased from 2000 to 2010, which was consistent with the results obtained by our research, and even exceeded the eastern coastal region and the northeast region from 2005 to 2010 [64–66]. The eastern megacities are faced with land shortage, rising land prices, and environmental degradation, so the state alleviates these problems through strict land approval [67]. In contrast, with the encouragement of the state, the northwest cities lag in development, but the expansion rate gradually exceeds that of the eastern coastal areas.

Since 2010, both central and local governments have introduced development strategies tailored to the provincial capitals of the five northwestern provinces. In Xi'an, efforts to protect the ecological environment led to the formulation of the "Qinling Ecological Environment Protection Plan", which restricted urban expansion to the south. The city also implemented the strategy of "eastward expansion, westward development, southern control, northern crossing, and central optimization", promoting coordinated development between Xi'an and surrounding cities [68,69]. In Urumqi, the 2014 Government Work Report outlined plans for the new North City District, and the city successfully hosted the Asia-Europe Expo and the Silk Road Economic Belt Urban Cooperation Forum in 2017, attracting investments totaling 296.6 billion yuan to drive urban development. Lanzhou gained approval from the State Council in 2012 to establish the first national-level new area, initiating northward expansion and addressing the challenge of limited development space. The local government of Lanzhou launched the "Remaking Lanzhou" strategy, expanding the urban planning area to 5810 square kilometers [70]. In 2018, the State Council approved the "Lanzhou-Xining Urban Agglomeration Development Plan", focusing on integrating into the Belt and Road Initiative, actively promoting high-quality development, and nurturing the Lanzhou-Xining urban agglomeration as a vital city cluster supporting national and ecological security in the northwest region [71]. Since then, the development of Lanzhou and Xining has entered a new phase, balancing urban development with ecological protection, providing opportunities for investment attraction, and actively driving urban development forward.

5.3. Some Suggestions for Regional Urban Construction and Planning

This paper analyzes the spatial morphological changes of the capital cities of the five provinces in Northwest China in the past 30 years and quantitatively evaluates the influence of various social and economic indicators on urban expansion. However, because policy factors are difficult to quantify, we cannot include them in a comprehensive quantitative analysis. Future research should strive to incorporate policy factors into the overall quantitative analysis framework. The urban expansion of the capital cities of the five provinces in northwest China is a typical example of urban development in western

China. These areas initially relied on economic and demographic support for development but were also constrained by topographical constraints. In Lanzhou, a typical solution is to develop new urban areas on suitable land. National and local policies should take into account the natural environment and topographical conditions of specific cities, link up with national strategic planning, adjust the intensity and direction of urban development according to the role and function of cities in regional development, and achieve more balanced inter-regional development.

6. Conclusions

This study took the capital cities of five provinces in China's underdeveloped northwestern region as its study sample. It used TM/OLI data from 1990 to 2020 as the information source, extracted the impervious surfaces of the five cities in each period based on the ENDISI and MNDWI indices, quantitatively analyzed them through a variety of urban form indicators such as the intensity of sprawl, sprawl pattern, direction of sprawl, and the migration of the city's center of gravity, and analyzed the factors influencing urban sprawl in terms of six first-level and eighteen second-level categories of indicators by means of the Geodetector software (version 1.0-4). The following conclusions were reached:

(1) From 1990 to 2020, the IS area of the five provincial capital cities increased year by year, but the intensity and area of expansion varied significantly from one period to another and from one city to another, with Xi'an having the largest expansion area, Xining having the highest expansion intensity, and Lanzhou expanding the least in terms of both area and intensity. During 1990–2000, the expansion of Xi'an and Urumqi was the largest, with expansion areas both greater than 80 km^2. From 2000 to 2010, the growth rate of expansion area and intensity in the five cities was extremely high, making this the most significant growth period in these three decades. Xi'an and Urumqi expanded by more than 100 km^2, and the other cities showed two- to fourfold growth. From 2010 to 2020, except for Urumqi, which maintained a continuous growth rate in urban expansion, the intensity of the other cities' expansion began to slow down, but their expansion areas remained large. The shift of the center of gravity of the five cities is affected by the topographic conditions in which they are located.

(2) From 1990 to 2020, the forms of the five cities become more decentralized, the shapes of city boundaries become more complex and irregular, and the directions of urban expansion diversified. Among them, Lanzhou experienced the greatest change, with a decrease of 54.46% in compactness and an increase of 4.98% in fractal dimension. Both Xi'an and Urumqi expanded to the northwest during 1990–2020. The center of gravity migration in Xi'an mainly occurred in 1990–2000, with a migration distance of 4.7 km; Urumqi, on the other hand, had a relatively large migration in 2000–2020, but experienced a northeasterly and then northwesterly migration direction, with a migration distance of 8.5 km. Lanzhou showed an overall trend of northward expansion, especially after 2000, with a migration distance of 23.7 km. Yinchuan and Xining differed in their direction of expansion, with Yinchuan migrating eastward and Xining migrating westward, and with the largest migration occurring from 2000 to 2010.

(3) From 1990 to 2020, the contribution rate of the same factor to different cities and different periods, as well as the contribution rate of different factors to the same cities and the same periods, differed significantly. During 1990–2000, economy and population were the main influencing factors of urban expansion, with the greatest influence in Xi'an, Urumqi, and Lanzhou, while natural factors had little impact on urban expansion. The contribution rate of each influencing factor to urban expansion increased during 2000–2010, with the most obvious increase in education and investment. Driven by the policy of Western development, the influence of economic factors on urban expansion in Yinchuan and Xining increased, the influence of population on urban expansion in Lanzhou declined, and the influence of natural factors was mainly reflected in Lanzhou and Xining. From 2010 to 2020, the contribution of living

standards, investment, and economy to urban expansion was further strengthened, and the influence of natural factors on Lanzhou was highlighted more significantly.

Author Contributions: Conceptualization, Wei Jia; methodology, Yuanbao Feng; software, Yuanbao Feng and Yujun Ma; validation, Xiangyu Hu, Sifa Shu and Hongda Li; formal analysis, Wei Jia; data curation, Yuanbao Feng; writing—original draft preparation, Yuanbao Feng; writing—review and editing, Wei Jia; supervision, Yujun Ma; project administration, Wei Jia. All authors have read and agreed to the published version of the manuscript.

Funding: This research was funded by the Natural Science Foundation of Qinghai Province of China (grant number 2021-ZJ-905).

Data Availability Statement: No new data were created or analyzed in this study. Data sharing is not applicable to this article.

Acknowledgments: We thank the NASA Earth Data Open Access for Open Science.

Conflicts of Interest: The authors declare no conflicts of interest.

Appendix A

Table A1. Details of the Landsat images used in this study areas.

City	Image Type	Image Data	Path/Row	Cloud Cover (%)
Xi'an	Landsat5 TM	07/04/1990	127/036	0
	Landsat5 TM	20/05/2000	127/036	0
	Landsat5 TM	26/12/2010	127/036	3
	landsat8 OLI	21/12/2020	127/036	0.69
Urumqi	Landsat5 TM	07/04/1990	143/029	1
	Landsat5 TM	07/04/1990	143/030	3
	Landsat5 TM	25/09/2000	143/029	3
	Landsat5 TM	25/09/2000	143/030	2
	Landsat5 TM	21/09/2010	143/029	0
	Landsat5 TM	20/08/2010	143/030	1
	landsat8 OLI	02/10/2020	143/029	0.31
	landsat8 OLI	02/10/2020	143/030	2.68
Lanzhou	Landsat5 TM	12/04/1990	130/035	1
	Landsat5 TM	18/03/1990	131/035	0
	Landsat5 TM	29/08/2000	130/035	12
	Landsat5 TM	21/09/2000	131/035	0
	Landsat5 TM	29/01/2010	130/035	1
	Landsat5 TM	05/02/2010	131/035	0
	landsat8 OLI	30/04/2020	130/035	3.87
	landsat8 OLI	17/02/2020	131/035	7.73
Yinchuan	Landsat5 TM	17/12/1990	129/033	0
	Landsat5 TM	28/12/2000	129/033	1
	Landsat5 TM	08/12/2010	129/033	2
	landsat8 OLI	01/11/2020	129/033	1.14
Xining	Landsat5 TM	22/12/1990	132/034	1
	Landsat5 TM	22/12/1990	132/035	1
	Landsat5 TM	17/12/2000	132/034	5
	Landsat5 TM	17/12/2000	132/035	3
	Landsat5 TM	29/12/2010	132/034	13
	Landsat5 TM	29/12/2010	132/035	2
	landsat8 OLI	24/12/2020	132/034	3.38
	landsat8 OLI	24/12/2020	132/035	1.87

References

1. WorldCities Report 2022: Envisaging the Future of Cities. Available online: https://unhabitat.org/world-cities-report-2022-envisaging-the-future-of-cities (accessed on 25 March 2024).
2. Lv, Y.; Chen, W.; Cheng, J. Effects of Urbanization on Energy Efficiency in China: New Evidence from Short Run and Long Run Efficiency Models. *Energy Policy* **2020**, *147*, 111858. [CrossRef]
3. Wang, W.-Z.; Liu, L.-C.; Liao, H.; Wei, Y.-M. Impacts of Urbanization on Carbon Emissions: An Empirical Analysis from OECD Countries. *Energy Policy* **2021**, *151*, 112171. [CrossRef]
4. Piano, E.; Souffreau, C.; Merckx, T.; Baardsen, L.F.; Backeljau, T.; Bonte, D.; Brans, K.I.; Cours, M.; Dahirel, M.; Debortoli, N.; et al. Urbanization Drives Cross-Taxon Declines in Abundance and Diversity at Multiple Spatial Scales. *Glob. Chang. Biol.* **2020**, *26*, 1196–1211. [CrossRef]
5. Zaryab, A.; Nassery, H.R.; Alijani, F. The Effects of Urbanization on the Groundwater System of the Kabul Shallow Aquifers, Afghanistan. *Hydrogeol. J.* **2022**, *30*, 429–443. [CrossRef]
6. Wu, W.; Li, C.; Liu, M.; Hu, Y.; Xiu, C. Change of Impervious Surface Area and Its Impacts on Urban Landscape: An Example of Shenyang between 2010 and 2017. *Ecosyst. Health Sustain.* **2020**, *6*, 1767511. [CrossRef]
7. Lu, D.; Weng, Q. Use of Impervious Surface in Urban Land-Use Classification. *Remote Sens. Environ.* **2006**, *102*, 146–160. [CrossRef]
8. Nowak, D.J.; Greenfield, E.J. The Increase of Impervious Cover and Decrease of Tree Cover within Urban Areas Globally (2012–2017). *Urban For. Urban Green.* **2020**, *49*, 126638. [CrossRef]
9. Zhang, H.; Lin, H.; Wang, Y. A New Scheme for Urban Impervious Surface Classification from SAR Images. *ISPRS J. Photogramm. Remote Sens.* **2018**, *139*, 103–118. [CrossRef]
10. Cao, X.; Gao, X.; Shen, Z.; Li, R. Expansion of Urban Impervious Surfaces in Xining City Based on GEE and Landsat Time Series Data. *IEEE Access* **2020**, *8*, 147097–147111. [CrossRef]
11. Weng, Q. Remote Sensing of Impervious Surfaces in the Urban Areas: Requirements, Methods, and Trends. *Remote Sens. Environ.* **2012**, *117*, 34–49. [CrossRef]
12. Zhang, X.; Liu, L.; Wu, C.; Chen, X.; Gao, Y.; Xie, S.; Zhang, B. Development of a Global 30 m Impervious Surface Map Using Multisource and Multitemporal Remote Sensing Datasets with the Google Earth Engine Platform. *Earth Syst. Sci. Data* **2020**, *12*, 1625–1648. [CrossRef]
13. Kuang, W.; Zhang, S.; Li, X.; Lu, D. A 30 m Resolution Dataset of China's Urban Impervious Surface Area and Green Space, 2000–2018. *Earth Syst. Sci. Data* **2021**, *13*, 63–82. [CrossRef]
14. Huang, X.; Li, J.; Yang, J.; Zhang, Z.; Li, D.; Liu, X. 30 m Global Impervious Surface Area Dynamics and Urban Expansion Pattern Observed by Landsat Satellites: From 1972 to 2019. *Sci. China Earth Sci.* **2021**, *64*, 1922–1933. [CrossRef]
15. Xu, H. Analysis of Impervious Surface and Its Impact on Urban Heat Environment Using the Normalized Difference Impervious Surface Index (NDISI). *Photogramm. Eng. Remote Sens.* **2010**, *76*, 557–565. [CrossRef]
16. As-syakur, A.R.; Adnyana, I.W.S.; Arthana, I.W.; Nuarsa, I.W. Enhanced Built-Up and Bareness Index (EBBI) for Mapping Built-Up and Bare Land in an Urban Area. *Remote Sens.* **2012**, *4*, 2957–2970. [CrossRef]
17. Deliry, S.I.; Avdan, Z.Y.; Avdan, U. Extracting Urban Impervious Surfaces from Sentinel-2 and Landsat-8 Satellite Data for Urban Planning and Environmental Management. *Environ. Sci. Pollut. Res.* **2021**, *28*, 6572–6586. [CrossRef]
18. Sekertekin, A.; Abdikan, S.; Marangoz, A.M. The Acquisition of Impervious Surface Area from LANDSAT 8 Satellite Sensor Data Using Urban Indices: A Comparative Analysis. *Environ. Monit. Assess.* **2018**, *190*, 381. [CrossRef]
19. Xu, G.; Dong, T.; Cobbinah, P.B.; Jiao, L.; Sumari, N.S.; Chai, B.; Liu, Y. Urban Expansion and Form Changes across African Cities with a Global Outlook: Spatiotemporal Analysis of Urban Land Densities. *J. Clean. Prod.* **2019**, *224*, 802–810. [CrossRef]
20. Xu, G.; Jiao, L.; Liu, J.; Shi, Z.; Zeng, C.; Liu, Y. Understanding Urban Expansion Combining Macro Patterns and Micro Dynamics in Three Southeast Asian Megacities. *Sci. Total Environ.* **2019**, *660*, 375–383. [CrossRef]
21. Dong, T.; Jiao, L.; Xu, G.; Yang, L.; Liu, J. Towards Sustainability? Analyzing Changing Urban Form Patterns in the United States, Europe, and China. *Sci. Total Environ.* **2019**, *671*, 632–643. [CrossRef]
22. Fu, B.; Peng, Y.; Zhao, J.; Wu, C.; Liu, Q.; Xiao, K.; Qian, G. Driving Forces of Impervious Surface in a World Metropolitan Area, Shanghai: Threshold and Scale Effect. *Environ. Monit. Assess.* **2019**, *191*, 771. [CrossRef]
23. Wu, W.; Zhao, S.; Henebry, G.M. Drivers of Urban Expansion over the Past Three Decades: A Comparative Study of Beijing, Tianjin, and Shijiazhuang. *Environ. Monit. Assess.* **2018**, *191*, 34. [CrossRef]
24. Petrişor, A.-I.; Hamma, W.; Nguyen, H.D.; Randazzo, G.; Muzirafuti, A.; Stan, M.-I.; Tran, V.T.; Aştefănoaiei, R.; Bui, Q.-T.; Vintilă, D.-F.; et al. Degradation of Coastlines under the Pressure of Urbanization and Tourism: Evidence on the Change of Land Systems from Europe, Asia and Africa. *Land* **2020**, *9*, 275. [CrossRef]
25. Luan, W.; Li, X. Rapid Urbanization and Its Driving Mechanism in the Pan-Third Pole Region. *Sci. Total Environ.* **2021**, *750*, 141270. [CrossRef]
26. Ma, Q.; He, C.; Wu, J. Behind the Rapid Expansion of Urban Impervious Surfaces in China: Major Influencing Factors Revealed by a Hierarchical Multiscale Analysis. *Land Use Policy* **2016**, *59*, 434–445. [CrossRef]
27. Ahmed, Z.; Asghar, M.M.; Malik, M.N.; Nawaz, K. Moving towards a Sustainable Environment: The Dynamic Linkage between Natural Resources, Human Capital, Urbanization, Economic Growth, and Ecological Footprint in China. *Resour. Policy* **2020**, *67*, 101677. [CrossRef]
28. Chen, Y.; Lee, C.C.; Chen, M. Ecological footprint, human capital, and urbanization. *Energy Environ.* **2022**, *33*, 487–510. [CrossRef]

29. Hoelscher, K.; Dorward, N.; Fox, S.; Lawanson, T.; Paller, J.W.; Phillips, M.L. Urbanization and Political Change in Africa. *Afr. Aff.* **2023**, *122*, 353–376. [CrossRef]
30. Hou, H.; Estoque, R.C.; Murayama, Y. Spatiotemporal Analysis of Urban Growth in Three African Capital Cities: A Grid-Cell-Based Analysis Using Remote Sensing Data. *J. Afr. Earth Sci.* **2016**, *123*, 381–391. [CrossRef]
31. Mao, F.; Li, X.; Zhou, G.; Huang, Z.; Xu, Y.; Chen, Q.; Yan, M.; Sun, J.; Xu, C.; Du, H. Land Use and Cover in Subtropical East Asia and Southeast Asia from 1700 to 2018. *Glob. Planet. Chang.* **2023**, *226*, 104157. [CrossRef]
32. Van Vliet, J. Direct and Indirect Loss of Natural Area from Urban Expansion. *Nat. Sustain.* **2019**, *2*, 755–763. [CrossRef]
33. Liao, K.; Huang, W.; Wang, C.; Wu, R.; Hu, Y. Spatio-Temporal Evolution Features and Impact Factors of Urban Expansion in Underdeveloped Cities: A Case Study of Nanchang, China. *Land* **2022**, *11*, 1799. [CrossRef]
34. United Nations. Human Development Report 2021-22. Available online: https://hdr.undp.org/content/human-development-report-2021-22 (accessed on 27 March 2024).
35. United Nations. Human Development Report 1990. Available online: https://hdr.undp.org/content/human-development-report-1990 (accessed on 27 March 2024).
36. United Nations. Human Development Report 2000. Available online: https://hdr.undp.org/content/human-development-report-2000 (accessed on 27 March 2024).
37. United Nations. Human Development Report 2010. Available online: https://hdr.undp.org/content/human-development-report-2010 (accessed on 27 March 2024).
38. United Nations. Human Development Report 2020. Available online: https://hdr.undp.org/content/human-development-report-2020 (accessed on 27 March 2024).
39. Grewal, B.S.; Ahmed, A.D. Is China's Western Region Development Strategy on Track? An Assessment. *J. Contemp. China* **2011**, *20*, 161–181. [CrossRef]
40. Wu, R.; Li, Z.; Wang, S. The Varying Driving Forces of Urban Land Expansion in China: Insights from a Spatial-Temporal Analysis. *Sci. Total Environ.* **2021**, *766*, 142591. [CrossRef]
41. China Statistical Yearbook 1990–2020. Available online: https://www.stats.gov.cn/sj/ndsj/ (accessed on 28 March 2024).
42. Earth Explorer. Available online: https://earthexplorer.usgs.gov/ (accessed on 28 March 2024).
43. Muñoz-Sabater, J.; Dutra, E.; Agustí-Panareda, A.; Albergel, C.; Arduini, G.; Balsamo, G.; Boussetta, S.; Choulga, M.; Harrigan, S.; Hersbach, H.; et al. ERA5-Land: A State-of-the-Art Global Reanalysis Dataset for Land Applications. *Earth Syst. Sci. Data* **2021**, *13*, 4349–4383. [CrossRef]
44. Chen, J.; Yang, K.; Chen, S.; Yang, C.; Zhang, S.; He, L. Enhanced Normalized Difference Index for Impervious Surface Area Estimation at the Plateau Basin Scale. *J. Appl. Remote Sens.* **2019**, *13*, 016502. [CrossRef]
45. Duan, P.; Zhang, F.; Liu, C. Extraction of the Impervious Surface of Typical Cities in Xinjiang Based on Sentinel-2A/B and Spatial Difference Analysis. Natl. *Remote Sens. Bull.* **2022**, *26*, 1469–1482. [CrossRef]
46. Tannier, C.; Thomas, I. Defining and Characterizing Urban Boundaries: A Fractal Analysis of Theoretical Cities and Belgian Cities. *Comput. Environ. Urban Syst.* **2013**, *41*, 234–248. [CrossRef]
47. Shen, G. Fractal Dimension and Fractal Growth of Urbanized Areas. *Int. J. Geogr. Inf. Sci.* **2002**, *16*, 419–437. [CrossRef]
48. Xu, J.; Zhao, Y.; Zhong, K.; Zhang, F.; Liu, X.; Sun, C. Measuring Spatio-Temporal Dynamics of Impervious Surface in Guangzhou, China, from 1988 to 2015, Using Time-Series Landsat Imagery. *Sci. Total Environ.* **2018**, *627*, 264–281. [CrossRef]
49. Chen, J.; Chang, K.; Karacsonyi, D.; Zhang, X. Comparing Urban Land Expansion and Its Driving Factors in Shenzhen and Dongguan, China. *Habitat Int.* **2014**, *43*, 61–71. [CrossRef]
50. Ma, Y.; Xu, R. Remote Sensing Monitoring and Driving Force Analysis of Urban Expansion in Guangzhou City, China. *Habitat Int.* **2010**, *34*, 228–235. [CrossRef]
51. Zhou, L.; Dang, X.; Mu, H.; Wang, B.; Wang, S. Cities Are Going Uphill: Slope Gradient Analysis of Urban Expansion and Its Driving Factors in China. *Sci. Total Environ.* **2021**, *775*, 145836. [CrossRef]
52. Tao, Y.; Ye, R. Analysis of the Spatio-Temporal Characteristics of Nanjing's Urban Expansion and Its Driving Mechanisms. *ISPRS Int. J. Geo-Inf.* **2022**, *11*, 406. [CrossRef]
53. Zhang, Z.; Luan, W.; Tian, C.; Su, M.; Li, Z. Spatial Distribution Equilibrium and Relationship between Construction Land Expansion and Basic Education Schools in Shanghai Based on POI Data. *Land* **2021**, *10*, 1059. [CrossRef]
54. Tian, L.; Li, Y.; Shao, L.; Zhang, Y. Measuring Spatio-Temporal Characteristics of City Expansion and Its Driving Forces in Shanghai from 1990 to 2015. *Chin. Geogr. Sci.* **2017**, *27*, 875–890. [CrossRef]
55. Jiang, L.; Deng, X.; Seto, K.C. Multi-Level Modeling of Urban Expansion and Cultivated Land Conversion for Urban Hotspot Counties in China. *Landsc. Urban Plan.* **2012**, *108*, 131–139. [CrossRef]
56. Wang, J.; Xu, C. Geodetector: Principle and prospective. *Acta Geogr. Sin.* **2017**, *72*, 116–134. [CrossRef]
57. Gong, P.; Li, X.; Zhang, W. 40-Year (1978–2017) Human Settlement Changes in China Reflected by Impervious Surfaces from Satellite Remote Sensing. *Sci. Bull.* **2019**, *64*, 756–763. [CrossRef]
58. Zhong, C.; Guo, H.; Swan, I.; Gao, P.; Yao, Q.; Li, H. Evaluating Trends, Profits, and Risks of Global Cities in Recent Urban Expansion for Advancing Sustainable Development. *Habitat Int.* **2023**, *138*, 102869. [CrossRef]
59. Gao, C.; Feng, Y.; Wang, R.; Lei, Z.; Chen, S.; Tang, X.; Xi, M. 50-Year Urban Expansion Patterns in Shanghai: Analysis Using Impervious Surface Data and Simulation Models. *Land* **2023**, *12*, 2065. [CrossRef]

60. Meng, L.; Sun, Y.; Zhao, S. Comparing the Spatial and Temporal Dynamics of Urban Expansion in Guangzhou and Shenzhen from 1975 to 2015: A Case Study of Pioneer Cities in China's Rapid Urbanization. *Land Use Policy* **2020**, *97*, 104753. [CrossRef]
61. Haas, J.; Ban, Y. Urban Growth and Environmental Impacts in Jing-Jin-Ji, the Yangtze, River Delta and the Pearl River Delta. *Int. J. Appl. Earth Obs. Geoinf.* **2014**, *30*, 42–55. [CrossRef]
62. Gong, J.; Hu, Z.; Chen, W.; Liu, Y.; Wang, J. Urban expansion dynamics and modes in metropolitan Guangzhou, China. *Land Use Policy* **2018**, *72*, 100–109. [CrossRef]
63. Xu, J.; Zhao, J.; Zhang, H.; Guo, X. Evolution of the Process of Urban Spatial and Temporal Patterns and Its Influencing Factors in Northeast China. *J. Urban Plan. Dev.* **2020**, *146*, 05020017. [CrossRef]
64. Zhang, X.; Pan, J. Spatiotemporal Pattern and Driving Factors of Urban Sprawl in China. *Land* **2021**, *10*, 1275. [CrossRef]
65. Li, G.; Sun, S.; Fang, C. The Varying Driving Forces of Urban Expansion in China: Insights from a Spatial-Temporal Analysis. *Landsc. Urban Plan.* **2018**, *174*, 63–77. [CrossRef]
66. Jing, S.; Yan, Y.; Niu, F.; Song, W. Urban Expansion in China: Spatiotemporal Dynamics and Determinants. *Land* **2022**, *11*, 356. [CrossRef]
67. Liu, Z.; Liu, S.; Qi, W.; Jin, H. Urban Sprawl among Chinese Cities of Different Population Sizes. *Habitat Int.* **2018**, *79*, 89–98. [CrossRef]
68. Xi'an Qinling Ecological Environment Protection Management Measures. Available online: https://www.moj.gov.cn/pub/sfbgw/flfggz/flfggzdfzwgz/201701/t20170122_141635.html (accessed on 29 March 2024).
69. Building the Next Trillion-Level Economic Carrier. Available online: http://www.xasw.gov.cn/info/1008/11687.htm (accessed on 29 March 2024).
70. Work Report of Lanzhou Municipal People's Government. 2012. Available online: https://www.lanzhou.gov.cn/art/2011/11/17/art_15361_899357.html (accessed on 29 March 2024).
71. The Ministry of Housing and Urban-Rural Development of the National Development and Reform Commission Issued a Notice on the Development Plan of Lanzhou-Xining Urban Agglomeration. Available online: https://www.ndrc.gov.cn/xxgk/zcfb/ghwb/201803/t20180319_962248.html (accessed on 29 March 2024).